Electronic control of soliton power transfer in silicon nanocrystal waveguides

Mengdi Li, Sergey A.Ponomarenko, Montasir Qasymeh and Michael Cada

Department of Electrical and Computer Engineering, Dalhousie University, Halifax, NS, B3J 2X4 Canada

serpo@dal.ca

Abstract: We demonstrate numerically that the power transfer from one polarization component of a $(1+1)$D vector spatial soliton to the other in a birefringent nonlinear medium can be controlled via the electro-optic Kerr effect by varying the externally applied electric field. We show how several all-optical operations involving fundamental vector solitons can be electronically controlled. We also discover that the split-up of the higher-order vector solitons due to the two-photon absorption (TPA) can be suppressed by adjusting the external electric field. The soliton trapping along the slow optical axis is realized by a planar waveguide, filled with a silicon-nanocrystal material. The external electric field is applied along the fast optical axis of the waveguide.

OCIS codes: (190.6135) Spatial solitons; (230.0250) Optoelectronics; (130.4815) Optical switching devices.

References and links

1. G. I. Stegeman and E. M. Wright, "All-optical waveguide switching," Opt. Quantum Electron. **22,** 95–122 (1990).
2. K. J. Blow, N. J. Doran, and D. Wood, "Polarization instabilities for solitons in birefringent fibers," Opt. Lett. **12,** 202–204 (1987).
3. M. Delque, D. Fanjoux, and T. Sylvestre, "Polarization dynamics of the fundamental vector soliton of isotropic Kerr media," Phys. Rev. E **75,** 016611 (2007).
4. U. Hempelmann, "Polarization coupling and transverse interaction of spatial optical solitons in a slab waveguide," J. Opt. Soc. Am. B **12,** 77–86 (1995).
5. For an up-to-date review see, Y. S. Kivshar and G. P. Agrawal, *Optical Solitons: From Fibers to Photonic Crystals* (Academic Press, Boston, 2003), Chapter 9.
6. J. S. Aitchison, J. U. Kang, and G. I. Stegeman, "Signal gain due to a polarization coupling in an AlGaAs channel waveguide," Appl. Phys. Lett. **67,** 2456–2458 (1995).
7. L. Thylen, "Integrated optics in $LiNbO_3$: Recent Developments in Devices for Telecommunications," J. Lightwave Technol. **6,** 847–861 (1988).
8. G. I. Stegeman, E. M. Wright, N. Finlayson, R. Zanoni, and C. T. Seaton, "Third Order Nonlinear Integrated Optics," J. Lightwave Technol. **6,** 953–970 (1988).
9. R. W. Boyd, *Nonlinear Optics* 2nd Edition (Academic Press, Amsterdam, 2003).
10. M. Cada , M. Qasymeh, and J. Pistora, "Electrically and optically controlled cross-polarized wave conversion," Opt. Express **16,** 3083–3100 (2008).
11. G. P. Agrawal, *Nonlinear Fiber Optics* 4th Edition (Academic Press, San Diego, 2007).
12. Q. Lin, O. J. Painter, and G. P. Agrawal, "Nonlinear optical phenomena in silicon waveguides: modeling and applications," Opt. Express **15,** 16604–16644 (2007).
13. J. M. Jarem and P. P. Banerjee, *Computational methods for electromagnetic and optical systems* (Marcel Dekker Inc., New York, 2000).
14. The Photonics Research Lab, University of Maryland, "SSPROP–Split-Step Fourier Propagation Software," http://www.photonics.umd.edu/software/ssprop/index.html.

#95045 - $15.00 USD Received 15 Apr 2008; revised 4 Jun 2008; accepted 5 Jun 2008; published 13 Jun 2008

15. G. V. Prakash, M. Cazzanelli, Z. Gaburro, L. Pavesi, F. Iacona, G. Franzò, and F. Priolo, "Nonlinear optical properties of silicon nanocrystals grown by plasma-enhanced chemical vapor deposition," J. Appl. Phys. **91,** 4607–4610 (2002).
16. F. Riboli, D. Navarro-Urrios, A. Chiasera, N. Daldosso, L. Pavesi, C. J. Oton, J. Heitmann, L. X. Yi, R. Scholz, and M. Zacharias, "Birefringence in optical waveguides made by silicon nanocrystal superlattices," Appl. Phys. Lett. **85,** 1268–1270 (2004).
17. S. M. Anthony, "Optical properties of nanostructured silicon-rich silicon dioxide," Thesis (Ph. D.)–Massachusetts Institute of Technology, Dept. of Materials Science and Engineering, (2006), Chapter 4.
18. J. S. Aitchison, A. M. Weiner, Y. Silberberg, D. E. Leaird, M. K. Oliver, J. L. Jackel, and P. W. E. Smith, "Experimental observation of spatial soliton interactions," Opt. Lett. **16,** 15–17 (1991).
19. V. V. Afanasjev, J. S. Aitchison, and Y. S. Kivshar, "Splitting of high-order spatial solitons under the action of two-photon absorption," Opt. Commun. **116,** 331–338 (1995).
20. V. Boucher, R. Barille, and G. Rivoire, "Polarization-switching control in a nonlinear liquid planar waveguide," J. Opt. Soc. Am. B **20,** 1666–1674 (2003).

1. Introduction

The operation of various all-optical devices, ranging from all-optical waveguide switches to distributed feedback couplers, relies on the power exchange among linearly and/or nonlinearly coupled optical fields [1]. A good deal of research has so far been carried out on the power transfer between the two (orthogonal) polarization components of vector spatial or temporal solitons, supported by nonlinear waveguides or fibers, respectively [2–5]. Nonlinear coupling of two orthogonally polarized beams has also been studied in connection with the signal amplification in AlGaAs channel waveguides [6]. In this case, not only are the two polarization components coupled via the cross-phase modulation, but they are also linearly coupled due to weak waveguide birefringence resulting from the waveguide design. Furthermore, as the directions of the fast and slow axes, assumed to correspond to the TE and TM polarizations, respectively, are fixed at the waveguide fabrication stage, the direction of the energy flow is also fixed. It is therefore only possible to amplify a weaker TE component at the expense of a stronger TM component. To reverse the energy flow direction, a $\pi/2$ phase difference between the two modes must be imposed.

To control the direction of the all-optical power transfer between the two orthogonally polarized modes of a waveguide or soliton polarization components, one could propose using the linear electro-optic effect by applying an electric field across the waveguide. Although the linear electro-optic effect in $LiNbO_3$ waveguides – a popular choice for integrated optics applications – has been thoroughly studied elsewhere [7, 8], it can only take place in nonlinear media with broken inversion symmetry [9]. The latter circumstance severely restricts the range of potential applications of the linear electro-optic effect to the optical power exchange control.

In this paper, we focus on a different possibility. As most optical materials exhibit the third-order nonlinearity, we propose to use the corresponding quadratic electro-optic effect to electronically control the power exchange between the vector spatial soliton components. Such an interesting emerging paradigm – controlling all-optical operations electronically [10] – can prove quite attractive for the future all-optical networks employing spatial solitons, as it is a relatively easy matter to adjust the properties of the electric fields.

In this work, we present the first proof-of-the-principle results and relegate the study of practical devices for the future. We will refer to the soliton component which acquires the power as the "signal" and the other soliton component as the "pump". In this language, we can realize the amplification of either a TE signal by a TM pump or a TM signal by a TE pump, regardless of the relative amplitudes of the TE and TM soliton components at the input. We demonstrate that the conversion efficiency of higher than 90% can be achieved for the fundamental vector solitons. Moreover, we show that the TPA-induced splitting of a high-order vector soliton into fundamental solitons can be suppressed by adjusting the magnitude of the external electric field.

#95045 - $15.00 USD Received 15 Apr 2008; revised 4 Jun 2008; accepted 5 Jun 2008; published 13 Jun 2008

Our analysis indicates that an "ideal" material for the realization of electronically controllable soliton power exchange must have a large third-order optical susceptibility coefficient such that the induced birefringence is comparable with the intrinsic modal birefringence. In addition, the "ideal" material must possess very small linear and nonlinear losses. We show that most of the desired functionalities can be realized employing a silicon-nanocrystal-based material.

This work is organized as follows. In Section 2, we show how the set of coupled $(1+1)$D nonlinear wave equations, governing the propagation of vector solitons in nonlinear waveguides, can be modified by including the external-field induced linear birefringence terms. In Section 3, we numerically investigate the electric field control of the all-optical power transfer from one component of the vector soliton to the other. We then present our conclusions in Section 4.

2. Theory

Consider an optical beam, propagating in an isotropic nonlinear medium in the planar waveguide geometry as indicated in Fig. 1. The beam propagation is mediated by an electric field E_{ext}, applied along the y-axis. The electric field of the optical beam can then be represented as

$$\mathbf{E} = \frac{1}{2}[\mathbf{a}_x \mathscr{E}_x e^{-i\omega_0 t} + \mathbf{a}_y(\mathscr{E}_y e^{-i\omega_0 t} + E_{ext})] + c.\,c. \tag{1}$$

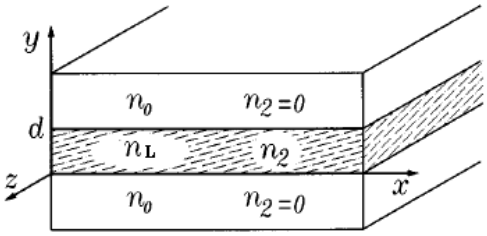

Fig. 1. Slab waveguide geometry (Ref. [4], Fig.1)

The dielectric response of the medium is assumed to be isotropic and of electronic origin. The third-order dielectric susceptibility tensor of any such medium is given by the expression [11]

$$\chi^{(3)}_{ijkl} = \frac{1}{3}\chi^{(3)}_{xxxx}(\delta_{ij}\delta_{kl} + \delta_{ik}\delta_{jl} + \delta_{il}\delta_{jk}). \tag{2}$$

The nonlinear polarization field, generated by any Kerr-type nonlinear medium, can be written as

$$\mathbf{P}_{NL} = \varepsilon_0 \chi^{(3)} \vdots \mathbf{EEE}. \tag{3}$$

It follows from Eq. (1) – (3) that the component of the polarization vector at an optical frequency ω_0 takes the form

$$\mathbf{P}_{NL} = \frac{1}{2}(\mathbf{a}_x \mathscr{P}_x + \mathbf{a}_y \mathscr{P}_y)e^{-i\omega_0 t} + c.\,c., \tag{4}$$

#95045 - $15.00 USD Received 15 Apr 2008; revised 4 Jun 2008; accepted 5 Jun 2008; published 13 Jun 2008

where

$$\mathscr{P}_x = \frac{3\varepsilon_0}{4}\chi^{(3)}_{xxxx}\left[(|\mathscr{E}_x|^2+\frac{2}{3}|\mathscr{E}_y|^2)\mathscr{E}_x+\frac{1}{3}(\mathscr{E}_x^*\mathscr{E}_y)\mathscr{E}_y+\frac{4}{3}E_{ext}^2\mathscr{E}_x\right], \quad (5)$$

$$\mathscr{P}_y = \frac{3\varepsilon_0}{4}\chi^{(3)}_{xxxx}\left[(|\mathscr{E}_y|^2+\frac{2}{3}|\mathscr{E}_x|^2)\mathscr{E}_x+\frac{1}{3}(\mathscr{E}_y^*\mathscr{E}_x)\mathscr{E}_x+4E_{ext}^2\mathscr{E}_y\right]. \quad (6)$$

In the derivation of Eqs. (5) and (6), we assumed the nonlinear dispersion to be small enough that the third-order optical susceptibility does not significantly depend on frequency in the spectral range of interest, implying that

$$\mathrm{Re}\{\chi^{(3)}_{xxxx}(-\omega_0,\omega_0,-\omega_0,\omega_0)\}\simeq\mathrm{Re}\{\chi^{(3)}_{xxxx}(-\omega_0,\omega_0,0,0)\}. \quad (7)$$

Throughout the rest of the paper, we also assume that the imaginary part of $\chi^{(3)}_{xxxx}(-\omega_0,\omega_0,0,0)$ is negligible, but the corresponding part of $\chi^{(3)}_{xxxx}(-\omega_0,\omega_0,-\omega_0,\omega_0)$ is not. The latter assumption holds true for many semiconductor materials for which the two-photon absorption processes, responsible for nonlinear losses, can play an important role in the frequency range $E_g<2\hbar\omega_0<2E_g$, where E_g is the band-gap energy [12].

The nonlinear wave equation, governing beam propagation, can be written in the form

$$\nabla^2\mathbf{E}-\frac{1}{\varepsilon_0c^2}\frac{\partial^2\mathbf{D}}{\partial t^2}=\mu_0\frac{\partial^2\mathbf{P}_{NL}}{\partial t^2}. \quad (8)$$

Here $\mathbf{D}=\varepsilon_0\mathbf{E}+\mathbf{P}_L$, where $\mathbf{P}_L=\varepsilon_0\chi_L\mathbf{E}$ is a linear polarization field. In the usual quasi-monochromatic and slow-varying envelope approximation, the solution to (8) in the waveguide geometry can be sought in the form

$$\mathscr{E}_j(x,z)=F(y)u_j(x,z)e^{i\beta_jz}, \quad (9)$$

where $F(y)$ is a spatial mode profile of the single-mode waveguide, $u_j(x,z)$ are slowly varying amplitudes of the components $j=x,y$. It is convenient to numerically analyze the optical power exchange in the circular polarization basis; the circular polarization components are related to the linear ones via the transformation

$$u_1=\frac{u_x+iu_y}{\sqrt{2}}e^{2i\kappa Z}; \qquad u_2=\frac{u_x-iu_y}{\sqrt{2}}e^{2i\kappa Z}. \quad (10)$$

Substituting from Eq. (9) into (8), averaging over the waveguide mode profile in a standard way [11], and making use of the transformation (10), we obtain a set of the coupled nonlinear wave equations for the circular polarization components in dimensionless (soliton) units:

$$\frac{\partial U_j}{\partial Z}+\frac{i}{2}\frac{\partial^2U_j}{\partial X^2}=-\tilde{\alpha}U_j+i\kappa U_{3-j}+\frac{2i}{3}\mathscr{N}^2(1+iK)(|U_j|^2+2|U_{3-j}|^2)U_j. \quad (11)$$

Here $j=1,2$ pertains to right (1) and left (2) circular polarizations, respectively. The dimensionless variables are $X=x/w_0$,$Z=z/L_D$, and $U_j=u_j(k_0L_Dn_2)^{1/2}$, where $k_0=\omega_0/c$. We have also introduced the notations: $L_D=\overline{\beta}w_0^2$ is a diffraction length, w_0 being a typical transverse beam size in the x-direction; $\overline{\beta}=(\beta_x+\beta_y)/2$, $n_2=3\mathrm{Re}\{\chi^{(3)}_{xxxx}\}/8n_L$ is the nonlinear refractive index, and $\tilde{\alpha}=\alpha L_D/2$ is a dimensionless linear loss coefficient.

The three key dimensionless parameters, defining the soliton dynamics, are the field-induced birefringence coefficient

$$\kappa=\frac{(\beta_x-\beta_y)L_D}{2}-\frac{4}{3}k_0n_2L_DE_{ext}^2, \quad (12)$$

#95045 - $15.00 USD Received 15 Apr 2008; revised 4 Jun 2008; accepted 5 Jun 2008; published 13 Jun 2008

a so-called soliton parameter, $\mathscr{N}$, defined as

$$\mathscr{N}^2 = L_D/L_{NL} = k_0^2 w_0 n_L n_{NL} p, \tag{13}$$

and a dimensionless TPA strength K specified as

$$K = \frac{\beta_{TPA} n_L}{2k_0 n_2}. \tag{14}$$

In Eqs. (13) and (14), p is a beam power (per unit length), and the two nonlinear refractive indices n_2 and n_{NL} are measured in different units and are related by $n_2 = n_{NL}\varepsilon_0 c n_L/2$ [11].

3. Numerical simulations

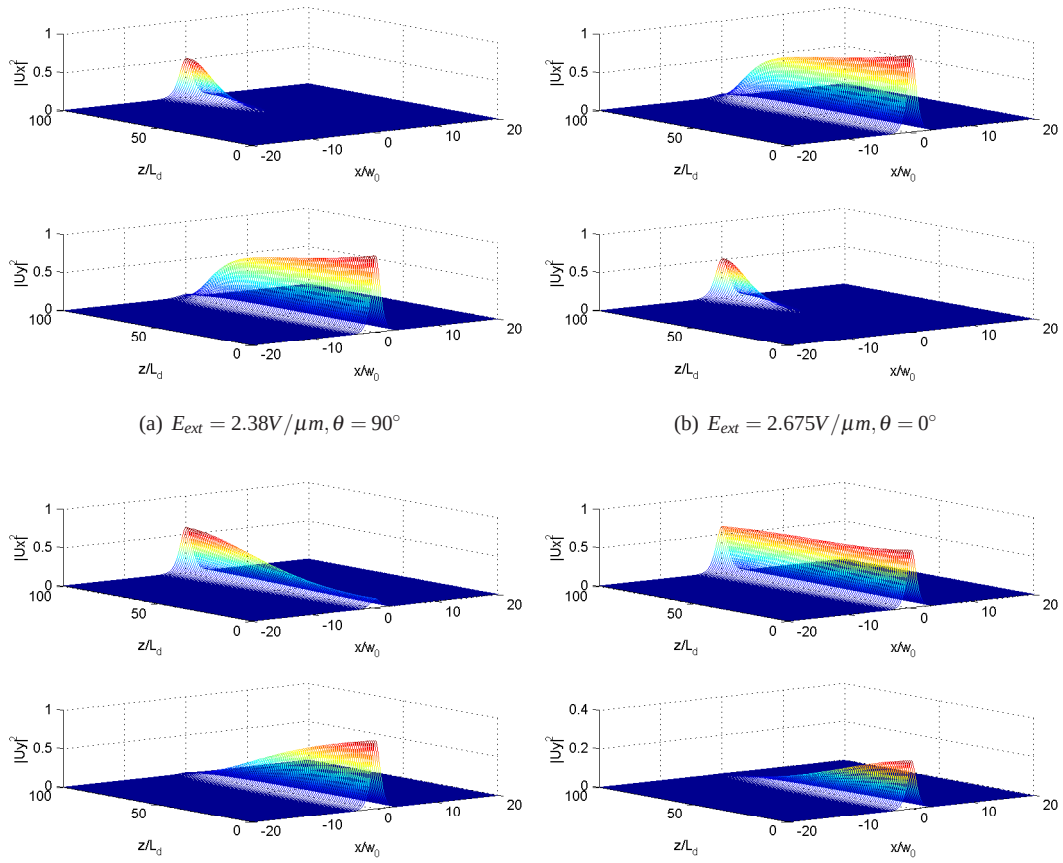

(a) $E_{ext} = 2.38V/\mu m, \theta = 90°$ (b) $E_{ext} = 2.675V/\mu m, \theta = 0°$

(c) $E_{ext} = 2.52V/\mu m, \theta = 70°$ (d) $E_{ext} = 2.527V/\mu m, \theta = 30°$

Fig. 2. Evolution of the intensity profiles of the fundamental vector soliton, $\mathscr{N}$ = 1, for different values of E_{ext} and θ. The dimensionless TPA strength is K = 0.0025.

We numerically solved Eq. (11) using a standard split-step Fourier method, which is commonly applied to the analysis of beam propagation problems [13]. In particular, we modified an open source code of SSPROP [14] by including the dc field-induced linear birefringence as

#95045 - $15.00 USD Received 15 Apr 2008; revised 4 Jun 2008; accepted 5 Jun 2008; published 13 Jun 2008

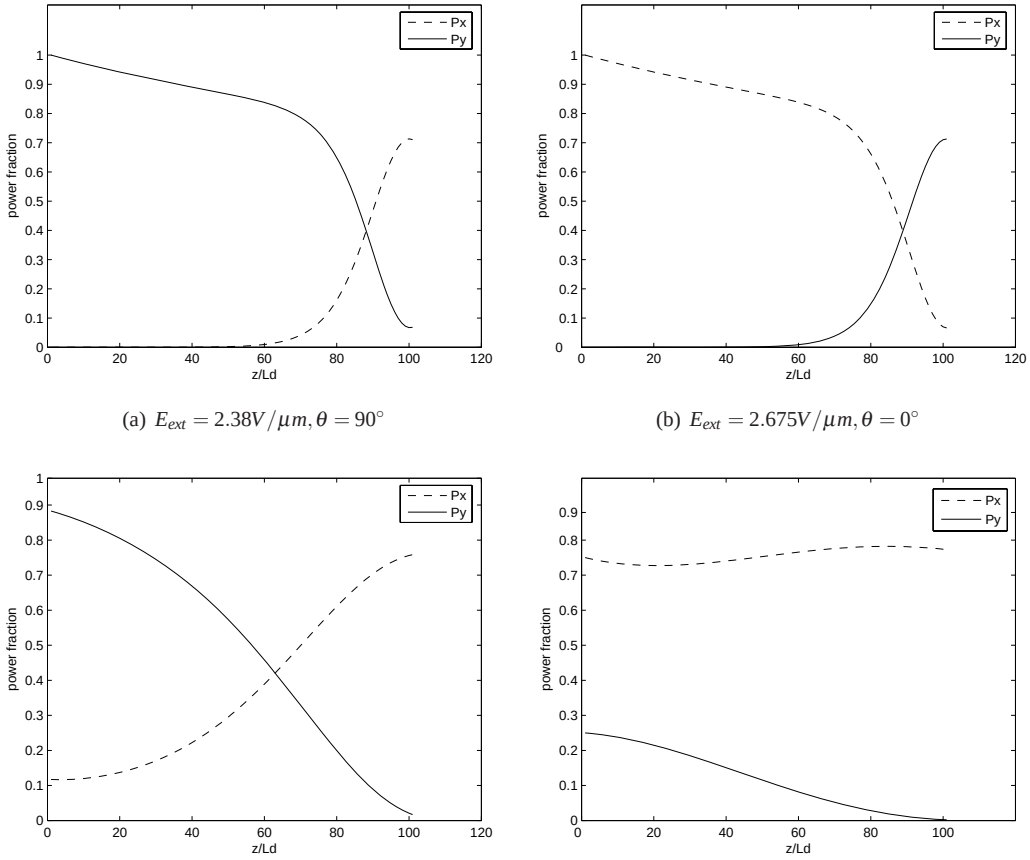

(a) $E_{ext} = 2.38V/\mu m, \theta = 90^\circ$

(b) $E_{ext} = 2.675V/\mu m, \theta = 0^\circ$

(c) $E_{ext} = 2.52V/\mu m, \theta = 70^\circ$

(d) $E_{ext} = 2.527V/\mu m, \theta = 30^\circ$

Fig. 3. Evolution of the powers of the fundamental vector soliton components, $\mathcal{N}$ = 1, for different values of E_{ext} and θ. The dimensionless TPA strength is K = 0.0025.

well as nonlinear loss terms. In our simulations, we have chosen silicon nanocrystals (Si-nc) as our nonlinear material due to its high nonlinear refractive index, $n_{NL} = 5.18 \times 10^{-15}$ m^2/W, and weak two-photon absorption, β_{TPA}=0.2 m/GW, both given at $\lambda_0 = 813$ nm [15]. Further, as the size of Si nanocrystals is much smaller than the wavelength of light, a Si-nc rich material usually has homogeneous optical properties and isotropic optical constants in the visible spectral range [16]. The magnitudes of the refractive index and the modal birefringence constant are influenced by many factors, such as Si content, the process of waveguide fabrication, etc. [17]. In this work, we used the following values of the parameters: λ_0=813nm, n_0=1.7, $\delta n = n_{TE} - n_{TM}$= 0.0002. For these values, the dimensionless TPA parameter is K = 0.0025. The input optical field had a hyperbolic secant profile (spatial soliton) with the beam waist $w_0 = 3\mu m$. The two orthogonally polarized components have zero phase difference (linear polarization), and the ratio of their amplitudes is specified by the angle θ that the soliton electric field makes with the slow axis of the waveguide. The external electric field was varied in the range from $0\,V/\mu m$ to $10\,V/\mu m$. The length of the waveguide was $100L_d$, which is about 1.11 cm.

#95045 - $15.00 USD Received 15 Apr 2008; revised 4 Jun 2008; accepted 5 Jun 2008; published 13 Jun 2008

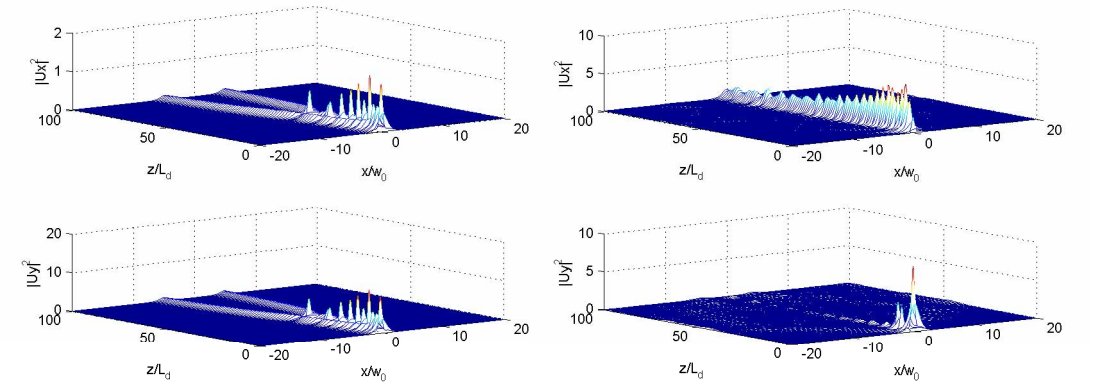

(a) $E_{ext} = 0V/\mu m, \theta = 70^\circ$ (b) $E_{ext} = 1.5V/\mu m, \theta = 70^\circ$

Fig. 4. Evolution of the intensity profiles of the second-order, $\mathcal{N}$ = 2, vector soliton, K = 0.0025 (a) in the absence of birefringence,i.e., $\Delta\beta$ = 0 (b) with internal birefringence and the external field present.

Whenever a single soliton-like beam, polarized along the y-axis (TM mode), is launched as shown in Fig. 2(a), one can set the external electric field to a certain value, equal to $2.38V/\mu m$ in our parameter regime, such that at the output almost all the power (96%) is switched to the x-component (TE mode), as is illustrated in Fig. 2(a) and 3(a). The total input power is chosen such that $\mathcal{N}$ = 1. Notice that since the power of the TM mode gradually decreases due to two-photon absorption, slightly less than 96% of the *incident* power is actually transferred to the TE mode. Similarly if a TE signal is initially launched as shown in Fig. 2(b), a TM polarized output can be amplified by simply setting the magnitude of the control field to $2.675V/\mu m$. This situation is illustrated in Fig. 2(b) and 3(b). Thus our numerical simulations demonstrate the possibility of designing a reconfigurable TE$\Longleftrightarrow$TM soliton mode converter.

If on the other hand, a vector soliton is launched as indicated in Fig. 2(c) and Fig. 2(d) such that $\mathcal{N}$ = 1, but one of the soliton components carries much more power than the other, the magnitude of the controlling electric field can be set to obtain either a weak signal amplification or a power limiting of a desired soliton component to a certain value. The former possibility is shown in Fig. 3(c), while the latter is illustrated in Fig. 3(d). It can be readily inferred by analyzing Fig. 2(d) and 3(d) that despite the nonlinear losses, the power-carrying polarization component loses only a negligible fraction of its initial power over the propagation distance of about 100 diffraction lengths, whereas the other component suffers a dramatic power loss over the same distance.

Finally, we consider a second-order soliton input, $\mathcal{N}$ = 2, where the TM component initially carries much more power than the TE one. The two-photon absorption will cause the amplitude and oscillation period of the second-order soliton decrease and increase, respectively, as it propagates down the waveguide until the soliton splits into a pair of fundamental solitons with equal amplitudes and different propagation angles. We display such an evolution scenario in Fig. 4(a) for the second-order soliton propagating without energy exchange, i.e., assuming no external control field and zero internal birefringence. We note that in the absence of the energy exchange between the higher-order *vector* soliton components, the TPA-induced soliton splitting in Kerr-like nonlinear media is qualitatively similar to the behavior of their *scalar* counterparts, which was studied experimentally in [18]. A comprehensive theoretical analysis of the TPA-induced

#95045 - $15.00 USD Received 15 Apr 2008; revised 4 Jun 2008; accepted 5 Jun 2008; published 13 Jun 2008

splitting of higher-order scalar solitons can be found in [19]. Such a splitting was characterized as a bifurcation-like phenomenon caused by non-adiabatic energy absorption at the point of the highest soliton field intensity, i.e., at the position of the strong soliton overlap.

The higher-order $\mathscr{N} = 2$, soliton evolution scenario qualitatively changes in presence of the birefringence-induced energy transfer between the polarization components of the vector soliton. In this case, as is evidenced in Fig. 4(b), there is power transfer, accompanied by slow (adiabatic) energy loss due to TPA, with the weaker polarization component transferring its power to the stronger one as well as to the medium. However, no soliton splitting occurs over the entire length of the waveguide, provided the magnitude of the electric field is set to a certain value. We conjecture that the suppression of the higher-order vector soliton splitting is a result of a subtle interplay between the periodic power exchange between the soliton components, whose period is controlled by the external dc field, and the action of the TPA. Indeed, as the peak intensity of the stronger soliton component is drastically reduced due to intensity-dependent two-photon absorption, the other component will transfer enough power to it to guarantee its structural integrity. Eventually, most of the power will reside in the slow-axis component which will then slowly (adiabatically) decay as a result of the TPA.

It should be noted that although we chose a specific input wavelength of 813 nm, all our numerical results remain qualitatively the same for any input wavelength as long as the nonlinearity is strong enough and the effect of TPA can not be neglected.

4. Conclusion

We have shown that an external electric field can be used to control, via the quadratic electro-optic effect, the power transfer between the components of a spatial vector soliton propagating in a planar waveguide filled with an isotropic Kerr-like nonlinear medium, i.e. Si-nc-based material. In particular, by adjusting both the external field applied along the fast axis of the waveguide, and the input polarization state of the soliton, one can switch the fast and slow axes of the waveguide and attain the maximum power transfer from the fast soliton component to the slow one. Thus, we have demonstrated that the application of the electric field can significantly affect the polarization dynamics of the vector soliton. Our simulation results can find diverse applications to such all-optical operations as the fanout implementation with a switching device [6], all-optical switching [1], power limiting [20], and optical routing, to mention just a few possibilities. It should be stressed here that we are reporting the first proof-of-principles results. Further research is needed to make the proposed functionalities attractive to the design of future electronically controllable all-optical switching/reconfigurable and/or multistable/storing devices.

#95045 - $15.00 USD Received 15 Apr 2008; revised 4 Jun 2008; accepted 5 Jun 2008; published 13 Jun 2008